1

Identification of COVID-19-relevant transcriptional regulatory networks and associated kinases as potential therapeutic targets

Chen Su[1], Simon Rousseau[2, *], and Amin Emad[1, *]

[1] Department of Electrical and Computer Engineering, McGill University, Montréal, QC, Canada

[2] The Meakins-Christie Laboratories at the Research Institute of the McGill University Heath Centre Research Institute, & Department of Medicine, Faculty of Medicine, McGill University, Montréal, QC, Canada

* Corresponding Author:

Amin Emad

755, McConnell Engineering Building

3480 University Street

Montreal, Quebec, Canada H3A 0E9

Email: amin.emad@mcgill.ca

Simon Rousseau

RI-MUHC, E M3.2244

1001 Décarie,

Montréal, Canada, H4A 3J1

Email: simon.rousseau@mcgill.ca

1

1   ABSTRACT

2   Identification of transcriptional regulatory mechanisms and signaling networks involved in the response

3   of host to infection by SARS-CoV-2 is a powerful approach that provides a systems biology view of gene

4   expression programs involved in COVID-19 and may enable identification of novel therapeutic targets

5   and strategies to mitigate the impact of this disease. In this study, we combined a series of recently

6   developed computational tools to identify transcriptional regulatory networks involved in the response

7   of epithelial cells to infection by SARS-CoV-2, and particularly regulatory mechanisms that are specific to

8   this virus. In addition, using network-guided analyses, we identified signaling pathways that are

9   associated with these networks and kinases that may regulate them. The results identified classical

10 antiviral response pathways including Interferon response factors (IRFs), interferons (IFNs), and JAK-

11 STAT signaling as key elements upregulated by SARS-CoV-2 in comparison to mock-treated cells. In

12 addition, comparing SARS-Cov-2 infection of airway epithelial cells to other respiratory viruses identified

13 pathways associated with regulation of inflammation (MAPK14) and immunity (BTK, MBX) that may

14 contribute to exacerbate organ damage linked with complications of COVID-19. The regulatory networks

15 identified herein reflect a combination of experimentally validated hits and novel pathways supporting

16 the computational pipeline to quickly narrow down promising avenue of investigations when facing an

17 emerging and novel disease such as COVID-19.

18

19   INTRODUCTION

20 Host responses to various insults is regulated by distinct sets of regulatory networks coordinating

21 responses matched to the insult. Viral infections of human cells lead to the production of interferons

22 (IFNs) as an antiviral mechanism [1]. TRIF, RIG-I and MDA-5-mediated activation of Interferon response

23 factors (IRFs) responsible for the expression of antiviral genes, such as type I, II and III IFNs, are amongst

24 critical regulators of antiviral immunity. In turn, Type I, II and III interferons will activate JAK-STAT signaling

25   to further promote antiviral host responses [2]. This response must be kept in balance as viral clearance

26   mechanisms can lead to tissue damage if not kept in check [3]. This balance can be especially hard to

27   maintain in the presence of new emerging infections such as the novel coronavirus severe acute

28   respiratory syndrome coronavirus - 2 (SARS-CoV-2) responsible for coronavirus disease 2019 (COVID-19),

29   for which the host is naïve. The loss of a measured response can lead to severe complications of viral

30   illnesses such as severe acute respiratory distress syndrome (ARDS), which has been observed in COVID-

31   19 patients [1].

32

33   Unraveling the gene expression programs involved in the response of the host to the infection by SARS-

34   CoV-2 can provide a fundamental understanding of COVID-19 and its complications and can enable

35   identification of therapeutic targets and novel treatments. The transcriptional regulatory network (TRN),

36   composed of transcription factors (TFs) and their target genes, play significant roles in regulating these

37   gene expression programs. Computational reconstruction of 'COVID-19-relevant' TRNs that depict

38   regulatory influence of TFs on genes differentially expressed due to infection of cells by SARS-CoV-2 would

39   facilitate our understanding of this disease. While comparing the transcriptomic profiles of cells infected

40   with SARS-CoV-2 with normal cells can provide some insight into the host response, understanding the

41   specific response that leads to ARDS and other complications prominent in COVID-19 requires evaluating

42   these molecular profiles against other respiratory viruses.

43

44   To identify transcriptional regulatory mechanisms involved in the host response to infection by SARS-CoV-

45   2, we analyzed gene expression profiles of human lung epithelial cell lines that were mock-treated or

46   infected by a respiratory virus (SARS-CoV-2, RSV, H1N1 and HPIV3) from a recent study [4]. SARS-CoV-2

47   (also named 2019 novel coronavirus (2019-nCoV) or human coronavirus 2019 (hCoV-19)) is a positive-

48   sense single-stranded RNA virus, part of the broad coronavirus family. Similar to SARS-Cov-1 and Middle

49   East respiratory syndrome (MERS), SARS-CoV-2 can cause severe acute respiratory disease in humans [1].

50   Respiratory syncytial virus (RSV) is a single-stranded negative-sense virus, a common cause of mostly mild

51   respiratory disease in children. However, both in children [5] and adults [3], it can lead to serious lung

52   diseases including ARDS. The influenza A virus H1N1, a negative-sense RNSA virus member of the

53   orthomyxoviridae family, that was responsible for the 2009 swine flu pandemic. Human parainfluenza

54   viruses (HPIV) are negative-sense RNA viruses that cause lower respiratory infections in children,

55   chronically ill and elderly patients [6].

56

57   First, using a computational tool that we recently developed for reconstruction of 'phenotype-relevant'

58   TRNs (InPheRNo) [7], we reconstructed COVID-19-relevant TRNs and identified key regulatory TFs

59   involved in the progress of the disease. TRNs are network representations of regulatory mechanisms in a

60   cell, in which nodes are TFs or genes, and each TF-gene edge represents a regulatory effect of the TF on

61   the gene. Unlike other methods for reconstruction of TRNs that are usually agnostic to the phenotype

62   under investigation, InPheRNo utilizes probabilistic graphical models to directly incorporate phenotypic

63   information in the TRN reconstruction. This approach enables identification of transcriptional regulatory

64   mechanisms that are involved in the specific phenotype under investigation by expression profiling (in

65   this study, response of cells infected by SARS-CoV-2 as compared to mock-treated cells or cells infected

66   by other viruses). Our results identified known and novel key regulatory TFs and signaling pathways

67   involved in COVID-19 and its associated complications.

68

69   Next, using a network-guided approach based on random walks on graphs, we identified kinases that

70   are most associated with the reconstructed COVID-19-relevant TRNs, as regulators of these networks

71   and potential therapeutic targets. Kinases are enzymes that are involved in the regulation of protein

72   activities through phosphorylation and are a major category of drug targets for human diseases. Using

4

73   data from gene knockdown experiments from the LINCS database [8], we observed that these kinases

74   indeed influence the expression of genes in the reconstructed TRNs in epithelial cells. Our analyses using

75   network-based algorithms and machine learning tools provided a systems biology perspective of the

76   response of the epithelial cells to infection by SARA-CoV-2 and identified regulatory mechanisms specific

77   to this virus. In addition, our results implicated important families of kinases (including JAK and MAPK

78   family) that may be used as therapeutic targets for COVID-19.

79

80   **RESULTS**

81   **COVID-19-relevant transcriptional regulatory networks implicate major transcription factors involved**

82   **in SARS-CoV-2 host response to infection**

83   We sought to identify transcriptional regulatory mechanisms involved in the host response to SARS-CoV-

84   2 infection. For this purpose, we obtained gene expression profiles of human lung epithelial cells that

85   were mock-treated or infected by SARS-CoV-2, respiratory syncytial virus (RSV), human parainfluenza

86   virus type 3 (HPIV3), influenza A/Puerto Rico/8/1934 (H1N1) virus (IAV), and IAV that lacks the NS1

87   protein (IAVdNS1) from a recent study [4]. The epithelial cells were Normal Human Bronchial Epithelial

88   (NHBE), transformed lung alveolar (A549), A549 cells transduced with a vector expressing human ACE2

89   (A549-ACE2), and Calu3 cells.

90

91   To identify COVID-19-relevant TRNs, we used InPheRNo [7], a method that we recently developed to

92   identify 'phenotype-relevant' TRNs using gene expression profiles of multiple samples and their

93   phenotypic labels. InPheRNo is based on a probabilistic graphical model (PGM) designed to integrate the

94   collective regulatory influence of multiple TFs on a gene with the association of the gene's expression

95   with a phenotype to identify regulatory mechanisms that are phenotype-relevant (as opposed to

96   phenotype-independent). In this approach, first the p-values of gene-phenotype associations (e.g. using

97   differential expression analysis) and p-values of gene-TF associations (using a two-step procedure based

98   on the Elastic Net algorithm) are obtained and provided as input 'observed variables' to the PGM. The

99   PGM is then trained on the data to obtain posterior probabilities for each TF-gene pair determining

100   whether the TF regulates the gene in a phenotype-relevant manner (details are provided in the original

101   manuscript [7]).

102

103   Using data corresponding to SARS-CoV-2 infected samples and their corresponding mock-treated

104   control, we first performed differential expression analysis and then reconstructed a COVID-19-relevant

105   TRN associated with SARS-CoV-2 infection (as compared to mock-treated samples) using 500 most

106   differentially expressed genes (FDR < 1.42E-3, shown in Supplementary Table S1), henceforth called

107   'SvM' (SARS-CoV-2 versus mock-treated). To also identify regulatory mechanisms that are specific to

108   SARS-CoV-2 infection (as opposed to infection by other viruses), we used InPheRNo to reconstruct a

109   COVID-19-relevant TRN using 500 differentially expressed genes (FDR < 1.43E-3, Supplementary Table

110   S1) by analyzing data corresponding to epithelial cells infected by SARS-CoV-2, IAV, IAVdNS1, RSV, and

111   HPIV3. Henceforth, we use 'SvOV' (SARS-CoV-2 versus other viruses) to refer to the second network. The

112   details of the analysis are provided in Methods and the reconstructed networks are provided in

113   Supplementary Table S2.

114

115   Given the SvM and SvOV COVID-19-relevant TRNs, we ranked TFs based on the number of COVID-19-

116   relevant target genes within each network. Tables 1-2 show the ranked list of top 8 TFs and top 21 TFs

117   that target at least 1% of the considered COVID-19-related genes in SvM and SvOV networks,

118   respectively (see Supplementary Table S3 for the full ranked list). We compared the targets of these TFs

119   identified by InPheRNo, with their targets determined using ChIP-seq data available in the Gene

120   Transcription Regulation Database (GTRD) database [9]. Three of the top 8 TFs in the SvM network

121   (NFKB1, STAT1, RELB) were present in the GTRD dataset. Out of the 18 targets identified by InPheRNo

122   for these TFs, 17 were confirmed by GTRD (p= 8.62E-07, hypergeometric test). Similarly, four of the top

123   TFs in the SvOV network (STAT1, RCOR1, EGR1, ZNF512B) were present in this dataset. Out of the 45

124   targets found for these TFs by InPheRNo, 37 were confirmed using GTRD (p = 2.36E-15, hypergeometric

125   test).

126

127   **Table 1:** Top 8 TFs implicated in the SvM (SARS-CoV-2 vs. mock-treated) network. The TFs are ranked based on the number of

128   their COVID-19-relevant target genes identified by InPheRNo. The second column shows the percent of the considered genes that

129   each TF regulates.

Transcription Factors	Percent of target genes
IRF9	3.05%
IRF7	1.96%
NFKB1	1.74%
MAFF	1.53%
SP110	1.09%
RELB	1.09%
STAT1	1.09%
BATF2	1.09%

130

131

132   Encouragingly, many of these TFs identified by InPheRNo have been previously shown to be activated

133   during COVID-19 or infections by other viruses. For example, Interferon regulatory factor 9 (IRF9), the

134   top hit in Table 1, was shown to be activated in SARS-CoV-2 infected NHBE cells [10]. While interestingly,

135   in contrast to observations with SARS-CoV-1, infection by SARS-Cov-2 failed to limit STAT1

136   phosphorylation [11], suggesting that STAT1 activity is maintained in SARS-CoV-2 CaLu-3 infected cells.

137

138

139

140 **Table 2:** Top 21 TFs implicated in the SvOV (SARS-CoV-2 vs. other viruses) network. The TFs are ranked based on the number of

141 their COVID-19-relevant target genes identified by InPheRNo. The second column shows the percent of the considered genes that

142 each TF regulates.

Transcription Factors	Percent of target genes
STAT1	5.89%
STAT2	2.95%
MLX	2.74%
EGR4	1.47%
RCOR1	1.47%
SP140L	1.47%
TP53	1.26%
RCOR2	1.26%
MAX	1.26%
ZNF496	1.26%
ZNF512B	1.05%
SMAD7	1.05%
SOX12	1.05%
IRF2	1.05%
HDX	1.05%
EGR1	1.05%
SP110	1.05%
IRF9	1.05%
ZNF143	1.05%
NFIX	1.05%
ZBTB32	1.05%

143

144 **Functional characterization of COVID-19-relevant TRNs implicate major signaling pathways involved in**

145 **the disease**

146 In order to determine the functional characteristics of gene expression programs involved in COVID-19,

147 we performed pathway enrichment analysis for the implicated TFs and their COVID-19-relevant target

148 genes in the SvM and SvOV networks. For this purpose, we used the gene set characterization (GSC)

149 computational pipeline of KnowEnG (Knowledge Engine for Genomics) analytical platform [12]. The GSC

150 pipeline enables 'standard' gene-set enrichment analysis (using Fisher's exact test), as well as advanced

151 'network-guided' analysis. The network-guided mode is an implementation of an algorithm called

152   DRaWR [13], which utilizes random walk with restarts (RWR) algorithm on a user-selected gene

153   interaction network to rank pathways based on their relevance to a query gene-set. Including a gene

154   interaction network (e.g. a protein-protein interaction (PPI) network) enriches the analysis and enables

155   identification of important pathways that may not be detectable using simple overlap-based Fisher's

156   exact test.

157

158   To this end, we used the set of top TFs in the SvM and SvOV networks (Tables 1-2) as separate query

159   sets and performed standard and network-guided (using experimentally verified PPI network from

160   STRING database [14]) pathway enrichment analysis (using Reactome pathways [15]) with default

161   parameters (Supplementary Table S4). Pathways related to cytokine signaling and interferon signaling

162   (interferon gamma signaling and interferon alpha/beta signaling) were implicated for both TRNs and

163   using standard and network-guided analysis. Next, we repeated the network-guided analysis above by

164   considering each TF and the set of its target genes in the SvM and SvOV networks as a separate query

165   gene set (Fig. 1 and Supplementary Tables S5-S6). Fig. 1 shows gene sets that are implicated for at least

166   two TFs and their targets in each TRN. Pathways related to Immune system, cytokines and interferon

167   signaling were again among the pathways implicated for the majority of TFs (and their COVID-19-

168   relevant targets).

169

170   **Identification of kinases associated with COVID-19-relevant TRNs as potential therapeutic targets**

171   Kinases are enzymes that are involved in the regulation of protein activities through phosphorylation

172   and are a major category of drug targets for human diseases [16]. Consequently, we sought to identify

173   human kinases that are most associated with the constructed COVID-19-relevant TRNs as important

174   signal transducers for this disease. For this purpose, we formed a kinase-substrate interaction (KSI)

175   network by aggregating kinase-substrate relationships from three previous studies [17-19] (see Methods

176   for details). The aggregated KSI contained 29594 kinase-substrate relationships corresponding to 406

177   unique kinases and 3942 unique substrates.

178

179   To identify kinases most associated with COVID-19 we used foRWaRD, a computational tool that we

180   recently developed to rank nodes and sets of nodes in a heterogenous network based on their relevance

181   to a set of query set using random walk with restarts (RWR) [20]. As input to foRWaRD, we provided the

182   aggregated KSI, a gene-gene interaction network (here we used HumanNet integrated network [21]),

183   and a query set containing the top TFs obtained from SvM TRN (8 TFs) and SvOV TRN (21 TFs),

184   separately. foRWaRD first forms a heterogenous network by superimposing the substrates on their

185   corresponding gene nodes in the gene-gene interaction network. Then, it performs two runs of the RWR

186   algorithm on this heterogenous network: one run with the query set (set of TFs) as the restart set and

187   another run with all nodes as the restart set (to be used as control). Each run of the RWR provides a

188   probability score for each node (including those corresponding to kinases), representing the relevance

189   of the node to the restart set. Finally, a normalized score for each kinase is obtained by comparing the

190   scores of the two runs of the RWR, and kinases are ranked based on how much their query set score is

191   higher than their background (i.e. control) score. Table 3 shows the 15 highest ranked kinases for the

192   top TFs corresponding to the SvM network and top TFs corresponding to the SvOV network,

193   respectively. The full ranked lists of kinases are provided in Supplementary Table S7. Figs. 2 and 3 show

194   network representations of the interactions among these kinases, their substrates, and the COVID-19-

195   relevant TRNs. Fig. 2 only includes direct kinase-TF interactions, while Fig. 3 and Supplementary Table S8

196   include indirect interactions of kinases and TFs.

197

198   As can be seen in Table 3, several families of kinases are implicated in both networks. JAK1, JAK2, and

199   JAK3, which are identified among the top 15 kinases for both SvM and SvOV TRNs, belong to the Janus

200   kinase family, a family of non-receptor tyrosine kinases [22]. This family of kinases are involved in the

201   transduction of cytokine-mediated signals through the JAK-STAT pathway. The members of the Janus

202   family and the JAK-STAT pathway have been suggested as potential therapeutic targets in COVID-19 [23-

203   26], supporting the validity of the results from this analysis.

204

205   **Table 3:** Top 15 kinases identified using foRWaRD for the top TFs in SvM and SvOV networks. The kinases are ranked based on

206   the ratio of their query set probability score to their background probability score. Any ratio score >1 implies that the kinase is

207   scored higher using the top TF query set compared to its control.

Ranked list of Kinases (based on top 8 TFs in SvM network)		Ranked list of Kinases (based on top 21 TFs in SvOV network)	
Kinase	**Ratio Score**	**Kinase**	**Ratio Score**
JAK2	45.76	MYO3A	11.60
IKBKE	26.20	JAK3	10.74
MAP2K5	23.88	VRK3	10.34
CHUK	17.17	ADCK1	9.74
IKBKB	14.22	JAK1	8.69
JAK3	10.47	MAP2K5	8.19
PRKDC	9.12	BMX	7.97
LIMK2	8.26	HIPK4	7.48
FGFR3	8.24	JAK2	7.46
RIPK1	7.89	MAP3K13	7.34
JAK1	7.48	LCK	6.63
IRAK1	6.48	CAMK2B	6.34
FLT1	5.66	MAPK14	6.32
MAP3K8	5.54	BTK	6.13
TBK1	5.28	MAPK11	6.05

208

209

210   **Evaluation of the predicted kinase-gene relationships using gene knockdown experiments**

211   Since foRWaRD incorporates both direct and indirect interactions to identify kinases, we sought to

212   determine whether the knockdown of identified kinases directly influence the expression of the TFs and

213   their target genes in the COVID-19-relevant TRNs. To this end, we obtained gene expression signatures

214   corresponding to shRNA knockdown experiments from the LINCS dataset [8]. We only focused on

11

215   experiments performed in A549 cell line, since it is one of the cell lines used in our analysis to construct

216   the COVID-19-relevant TRNs and a cell line shown to be susceptible to SARS-CoV-2 infection [27]. The

217   gene expression signatures correspond to z-score normalized changes in the expression of 978 'L1000

218   landmark genes' as a result of knockdown of a single gene, when compared to control (no knockdown).

219   We defined a landmark gene to be positively (or negatively) influenced by the knockdown of a kinase if

220   its expression increased (decreased) as a result of the knockdown and also if its normalized expression

221   change was among the top (bottom) 15% of all landmark genes.

222

223   Out of the 15 kinases implicated using foRWaRD for the SvM analysis, shRNA knockdown signatures in

224   A549 cells were available for 13 of them. In addition, 10 target genes and 2 TFs from the SvM TRN were

225   among the L1000 landmark genes whose expression change were measured. All of the 2 TFs and the 10

226   target genes were positively or negatively influenced by the knockdown of at least one of the implicated

227   kinases (Supplementary Table S9 and Supplementary Figures S1-S2), supporting the interactions

228   discovered in this study.

229

230   We repeated the analysis above using the kinases implicated for the SvOV network. Knockdown

231   signatures were only available for 7 (out of 15) implicated kinases. In addition, 14 target genes and 3 TFs

232   from the SvOV TRN were among the L1000 landmark genes. Our analysis showed that 12 target genes

233   (out of 14) and 2 TFs (out of 3) were positively or negatively influenced by the knockdown of at least one

234   of the 7 kinases (Figure 4, Supplementary Table S9 and Supplementary Figure S3). Figure 4 shows the

235   histogram of the expression changes of the landmark genes as a result of each kinase knockdown and its

236   effect on the TFs and target genes in the SvOV TRN.

237

238   Taken together, these results show that our computational pipeline that strings together InPheRNo,

239   KnowEnG's GSC, and foRWaRD is capable of identifying biologically plausible signaling networks involved

240   in regulating the responsible of airway epithelial cells to SARS-CoV-2.

241

242   **DISCUSSION and CONCLUSION**

243   The aim of this study was to identify signaling and transcriptional regulatory networks that play key roles

244   in transducing signals specific to SARS-CoV-2 infection of airway epithelial cells in order to better

245   understand the pathophysiology of COVID-19 and provide a list of potential molecular targets for

246   therapies aimed at altering the clinical courses of the disease. The response was studied in comparison

247   to mock-treated cells and other viruses (RSV, H1N1, HPIV3).

248

249   *Insights learned from the regulatory networks associated with SARS-CoV-2 versus mock-treated cells:* In

250   the first instance, comparing to mock-treated cells, we can identify the key regulatory pathways of

251   antiviral responses. Alterations of these pathways (whether genetic, epigenetic or environmental) can

252   have important consequences for a broad range of infections. If their activity is diminished or impaired,

253   susceptibility to viral infections is expected, with high titers of virus likely increasing infectivity. This is

254   the case for the loss of function of TLR7 [28] or type I and type III IFN-related genes [29, 30] leading to

255   more severe COVID-19 disease in younger individuals. As expected, pathway enrichment analysis

256   showed that immune (cytokine) signaling related to interferon were the top hits, as is expected for viral

257   infection of host cells [31]. Amongst the lists of TFs identified is IRF9, a TF shown to be activated by

258   SARS-CoV-2 [10] that forms a trimeric complex with STAT1 and STAT2 termed IFN-stimulated gene factor

259   3 (ISG3) that binds to the IFN stimulated response element (ISRE) and controls the expression of type I

260   and III IFN essential for the control of Influenza A virus replication [32]. Interferons alpha and beta (IFN-a

261   and IFN-b) are among the type I IFNs that regulate the activity of immune system and act as antiviral

262   cytokines. A recent study has shown an association between impaired interferon type I response

13

263   (represented by low activity of IFN-a and IFN-b) and severity of COVID-19 and has suggested blood

264   deficiency in type I IFN as a hallmark of severe manifestation of the disease [28]. In addition, several

265   studies have suggested type I IFNs as potential antiviral treatments for COVID-19 [29, 30]. IFN-g is a

266   cytokine involved in innate and adaptive immunity and is the only member of type II IFNs. A recent study

267   has shown a correlation between COVID-19 severity and a decrease in the production of IFN-g by CD4+ T

268   cells [31].

269

270   Pathway enrichment provides a high-level view, which lacks granular information about the regulatory

271   pathways involved. For this reason, we focused our analysis on linking protein kinases to the identified

272   network using foRWaRD. This analysis confirmed the importance of JAK-STAT and NFkB signaling for the

273   expression of IFN genes and antiviral responses in SARS-CoV-2 versus mock-treated cells (Fig. 2A and

274   3A). Identified kinases also included TANK-binding kinase 1 (TBK1) and IKKe, critical regulators of the

275   transcription factor IRF7 that regulate amongst other genes IFN-induced oligodenylate synthetase-like

276   (OASL) and Pentraxin-3 (PTX3) (Fig. 2A). TBK1/IKKe acts downstream of TLR3 and TLR7 via the TRIF-

277   signaling adapter, two TLR identified in genetic studies to confer susceptibility to COVID-19 [33, 34].

278   Moreover, high circulating expression of PTX3, derived from monocytic and endothelial cells is a

279   predictor of short-term COVID-19 mortality [35]. The analysis thus identified several relevant pathways

280   to SARS-CoV-2 infection and disease susceptibility/severity.

281

282   *Insights learned from the regulatory networks associated with SARS-CoV-2 versus other respiratory virus-*

283   *treated cells:* Investigation of the regulatory networks specifically associated with SARS-CoV-2 can help

284   better understand either acute complications or long-term consequences of COVID-19. This is

285   particularly important for a novel disease, for which limited information is available. Considering that

14

286   as of December 2020, more than 75 million people have been infected, the potential of diverging

287   responses is huge and can have long-lasting impact on the health of many. Therefore, better

288   understanding the peculiarities of SARS-CoV-2 compared to other viruses is paramount to deal with the

289   coming fall out of the pandemic. When looking at differences between mock- and other viruses-treated

290   cells, the enrichment analysis highlighted a potential role for GPCR signaling associated with the TFs

291   MAX, SP110 and EGR4. GPCRs form a large family of 7-transmembrane cell surface receptors that

292   mediates numerous cellular functions, including cytokine/chemokine signaling involved in leukocyte

293   chemotaxis [36]. The association with the above-mentioned TFs postulate a role in controlling cell

294   differentiation/cell death programs by GPCR.

295

296   In the SvOV network, additional protein kinases were identified including MAPK11, MAPK14, BTK, and

297   BMX. MAPK11 and MAPK14 both belong to the p38 MAPK family which are involved in the cellular

298   responses to extracellular stimuli including proinflammatory cytokines such as IL-6 [37]. Previously, it

299   has been shown that one of the proteins expressed by SARS-CoV virus upregulates p38 MAPK [38]. A

300   global phosphorylation analysis of SARS-CoV-2 infected epithelial cells also identified MAPK14 and

301   MAPK11 as kinases upregulated during infection that make important contributions to host responses

302   [39]. Accordingly, inhibition of MAPK14 and MAPK11 family has been proposed as a potential

303   therapeutic approach in COVID-19 [37]. In addition to be a downstream target of TLR-signaling pathways

304   including TLR3 in airway epithelial cells [40], MAPK14 regulates IL-6 expression and mRNA stability [41].

305   IL-6 circulating levels are elevated in severe COVID-19 [42]. Moreover, MAPK14 is an important signal

306   transducer of IL-17 in endothelial cells [43], involved in neutrophilic inflammation, that may be

307   important mediators of thrombosis in COVID-19 via the release of Neutrophil-Extracellular-Traps [20,

308   44]. MAPK14 is an important target of the potent corticosteroid dexamethasone [45], that was shown to

309   decrease mortality in severe COVID-19 [46].

310

311 BMX and BTK are non-receptor tyrosine kinases that belong to the Tec kinase family. Tec family has

312 been shown to be involved in the intracellular signaling mechanisms of cytokine receptors and antigen

313 receptor signaling in lymphocytes [47]. BMX has been shown to link both MYD88, another TLR-signaling

314 adapter, and Focal Adhesion Kinases, a kinase associated with integrin activation to the synthesis of IL-6

315 [48]. The inhibition of genes in this family, and particularly BTK [41], has been proposed as a therapeutic

316 approach to protect COVID-19 patients against pulmonary injury [42] and to block thrombo-

317 inflammation [43]. Two potential downstream targets of BTK according to our regulatory networks (Fig.

318 2B), Tumor necrosis factor ligand superfamily member 14 (TNFS14) and XIAP-associated factor 1 (XAF1)

319 have been identified in a single cell transcriptomic study comparing IAV and SARS-CoV-2 responses [49].

320 TNFSF14 is a ligand of the lymphotoxin beta receptor that amplifies NFkB signaling in T lymphocytes to

321 increase IFN-gamma production [50]. XAF1, as its name implies, binds XIAP (BIRC4) an important

322 regulator of inflammatory signaling and apoptosis, that increases TRAIL-mediated apoptosis in response

323 to IFNb [51]. While these responses are likely desirable during early phases of the infection, whether

324 they can also contribute to immunopathology in the second sustained phase of the disease warrants

325 further investigation.

326

327 In conclusion, our results obtained by stringing together three powerful computational tools (InPheRNo,

328 KnowEnG GSC, and foRWaRD) identified regulatory networks, pathways, and kinases, many of which

329 have already been associated with COVID-19 in previous studies. These results also provided further

330 information on putative regulatory mechanisms underpinning the infection of epithelial cells by SARS-

331 CoV-2 and identified novel potential therapeutic targets that can serve as the basis for future

332 identification and development of drugs that mitigate the impact of COVID-19 in individuals at risk of

333 severe complications. The SvM regulatory network was mostly related to classic antiviral response

16

334   pathways (IRF, IFN, JAK-STAT, etc.) that are well supported by genomic data on diseases susceptibility to

335   COVID-19 [33, 34]. Interestingly, the SvOV regulatory network identified pathways associated with

336   regulation of inflammation (MAPK14) and immunity (BTK, BMX) that may contribute to exacerbate

337   organ damage.

338

339   **METHODS**

340   **Data collection**

341   We downloaded mock-treated and infected RNA-seq gene expression profiles of human lung epithelial

342   cells from the Gene Expression Omnibus (GEO) database (accession number: GSE147507). For the

343   reconstruction of SARS-CoV-2 versus mock (SvM) TRN, we used 24 samples corresponding to

344   independent biological triplicates of SARS-CoV-2 infected NHBE, A549, A549-ACE2, and Calu3 and their

345   corresponding mock-treated control. For the reconstruction of SARS-CoV-2 versus other viruses (SvOV)

346   TRN, we used 33 samples corresponding to independent biological replicates of A549 cells infected with

347   SARS-CoV-2, RSV, IAV, and HPIV3, NHBE cells infected with SARS-CoV-2, IAV, and IAVdNS, A549-ACE2

348   cells infected with SARS-CoV-2, and Calu3 cells infected with SARS-CoV-2.

349

350   We downloaded the list of human TFs from AnimalTFDB [52]. Experimentally verified protein-protein

351   interaction network from the STRING database [14] and HumanNet integrated network [21] were

352   downloaded from KnowEnG's knowledge network (version 17.06) available at the address

353   https://github.com/KnowEnG/KN_Fetcher/blob/master/Contents.md. The list of target genes for the

354   top TFs (identified using ChIP-seq) was downloaded from the GTRD database

355   (http://gtrd.biouml.org/downloads/20.06/intervals/target_genes/Homo%20sapiens/genes%20promote

356   r%5b-1000,+100%5d/). In this dataset, a gene is considered to be target of a TF if its promoter region

357   (defined as the interval [-1000, +100] bp relative to gene's transcriptional start site) contains at least one

358   GTRD meta-cluster for the TF. The meta-clusters reflect ChIP peaks for the same TF-gene but integrated

359   from different experiment conditions and different peak calling methods [9].

360

361   To form the aggregated KSI network, we obtained kinase-substrate relationships from three previous

362   studies. The interactions corresponding to homo sapiens were downloaded from PhosphoSitePlus

363   database (www.phosphosite.org) [17], PhosphoNetworks (www.phosphonetworks.org) [18], and the

364   supplementary material of an independent study [19]. After removing duplicate edges, we formed a KSI

365   involving 29594 kinase-substrate relationships corresponding to 406 unique kinases and 3942 unique

366   substrates. LINCS Level 5 consensus signatures ('trt_sh.cgs') corresponding to shRNA knockdowns in

367   A549 cell line were obtained from GEO with the accession number (GSE92742). We used the Consensus

368   Gene Signatures (CGS) data since they correspond to gene expression changes that are common among

369   multiple shRNAs that target the same gene, mitigating off-target effects [53].

370

371   **Reconstruction of COVID-19-relevant TRNs using InPheRNo**

372   InPheRNo [7] is a computational method that utilizes a probabilistic graphical model to combine

373   information on the significance (pseudo p-value) of gene-TF associations (from their expression profiles)

374   with information on the significance (p-value) of gene-phenotype associations to construct phenotype-

375   relevant TRNs. As input, it accepts a list of TFs, the expression profiles of genes and TFs (in multiple

376   samples), and the p-value of association between genes' expression and a phenotype.

377

378   To construct the TRNs using InPheRNo, we first performed differential expression analysis using EdgeR

379   [54] with the cell type as a confounding factor. In the case of SvOV, since for different viruses the

380   measurements were obtained at different time-points, we also included the time of measurement post

381   infection as a confounding factor. Next, we quantile normalized the gene expression profiles using voom

18

382   [55] and then z-score normalized the results. We constructed the SvM and SvOV TRNs using 500 most

383   differentially expressed genes. We ran InPheRNo (downloaded from

384   https://github.com/KnowEnG/InPheRNo) with 1000 iterations, 500 repeats and default values for other

385   parameters.

386

387   **Pathway enrichment analysis**

388   We used KnowEnG's gene set characterization (GSC) pipeline [12] (www.knoweng.org/analyze) to

389   perform pathway enrichment analysis. For the standard mode of GSC pipeline (without use of any gene

390   interaction network), we chose Reactome pathways [15] as the option for target gene sets and the rest

391   of parameters were left as default. We excluded pathways with smaller than 10 genes and adjusted the

392   enrichment p-values (Fisher's exact test) for multiple tests using Benjamini-Hochberg false discovery

393   rate (FDR). Pathways with FDR < 0.05 were considered statistically significant.

394

395   For the knowledge-guided mode of the GSC pipeline, we used 'STRING Experimental PPI' option for the

396   knowledge network (which corresponds to experimentally verified protein-protein interaction edges

397   from the STRING database [14]) and the amount of network smoothing was set to the default 50%. Only

398   pathways with 'difference score' larger than 0.5, which correspond to those that have a query score

399   higher than the background score, were considered associated with the input query gene set. For

400   enrichment analysis of the set of TFs, the input file to KnowEnG's GSC pipeline was designed such that

401   the universe (i.e. population) would be equal to the set of all TFs present in our study. For enrichment

402   analysis of a TF and its target genes, the universe was set to be the set of all genes and TFs present in

403   our study.

404

405

19

406 **Authors' Contributions**

407 AE and SR conceived the study. CS performed the analyses. All authors contributed to the drafting of the

408 manuscript and critical discussion of the results. All authors read and approved the final manuscript.
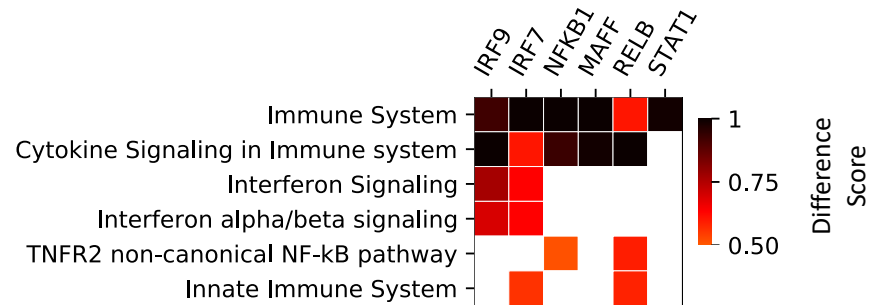
409

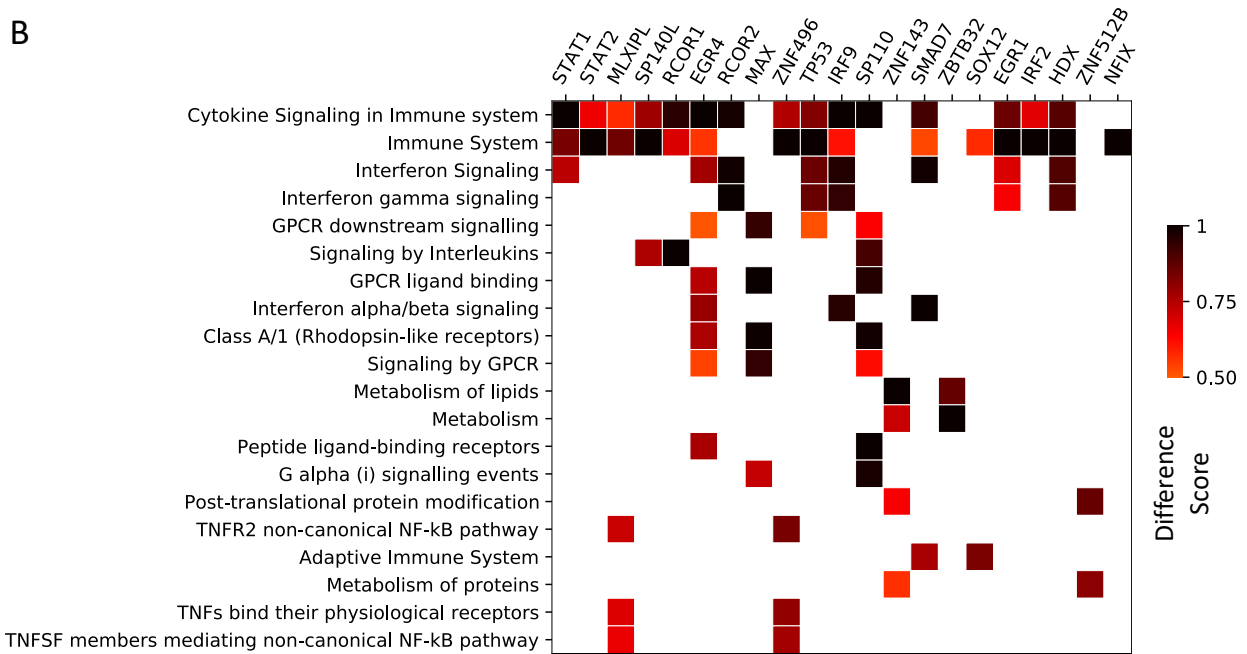410 **Acknowledgements**

413

414 **Competing Interests**

415 The authors declare no conflict of interest.

416

417

Figure Legends:

419

Figure 1: Pathway enrichment analysis using network-guided gene set characterization pipeline of

KnowEnG. The columns correspond to top TFs and their COVID-19-relevant targets identified using

InPheRNo. Only pathways that have been implicated for at least two TFs (and their targets) are depicted

(see Supplementary Tables S5 and S6 for the full list). The heatmap shows the 'difference score'

assigned to each pathway using KnowEnG. Cases in which the score was <0.5 are shown as white. A)

Implicated pathways for top TFs in the SvM TRN. B) Implicated pathways for top TFs in the SvOV
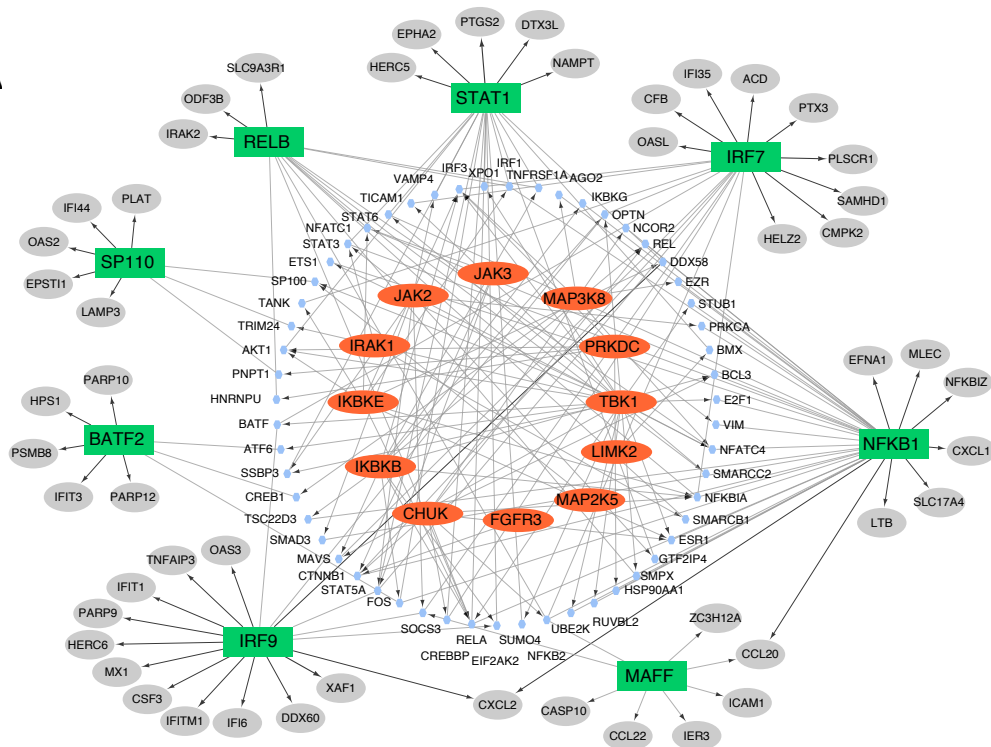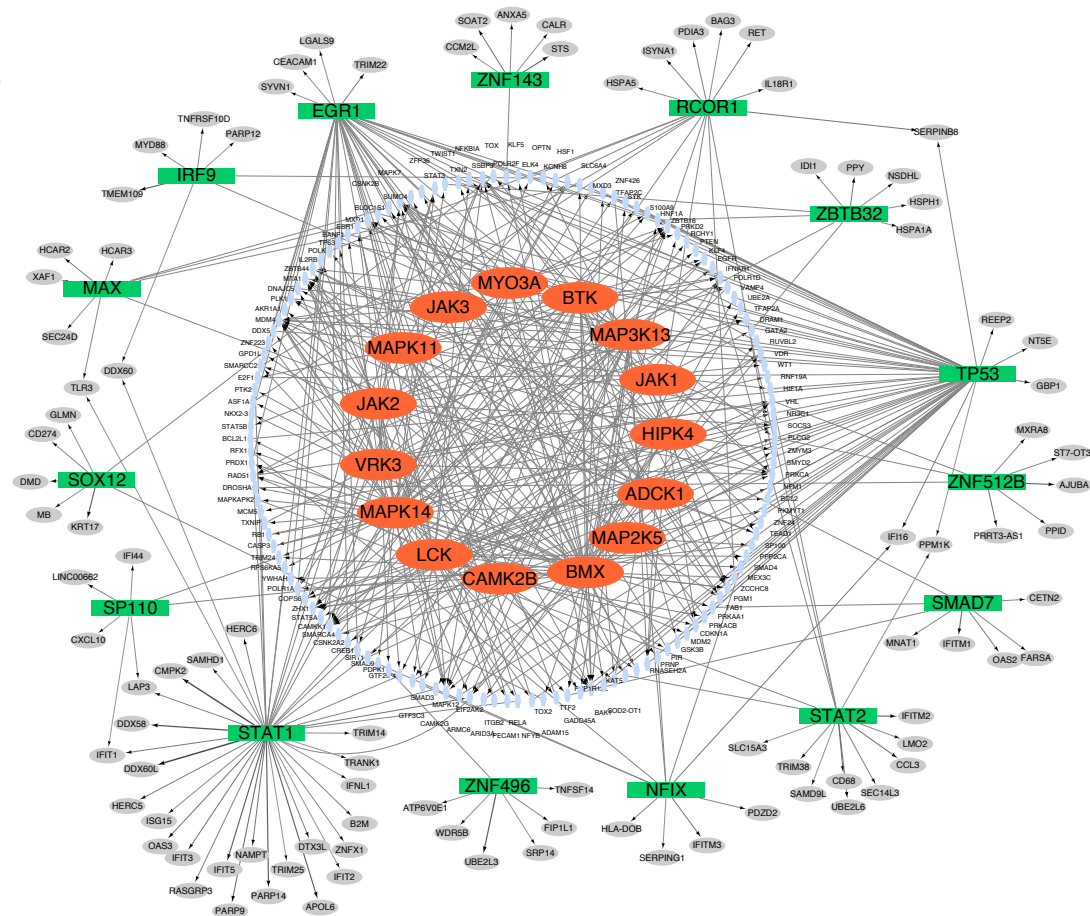
network.

427
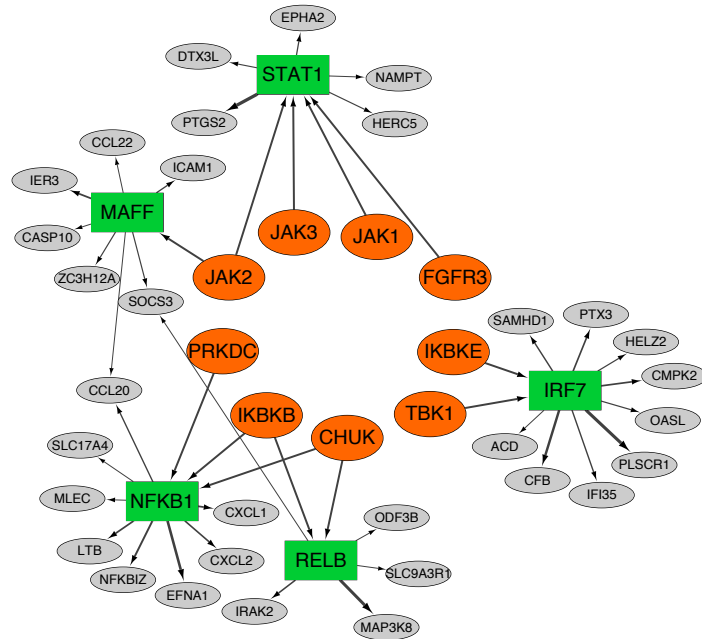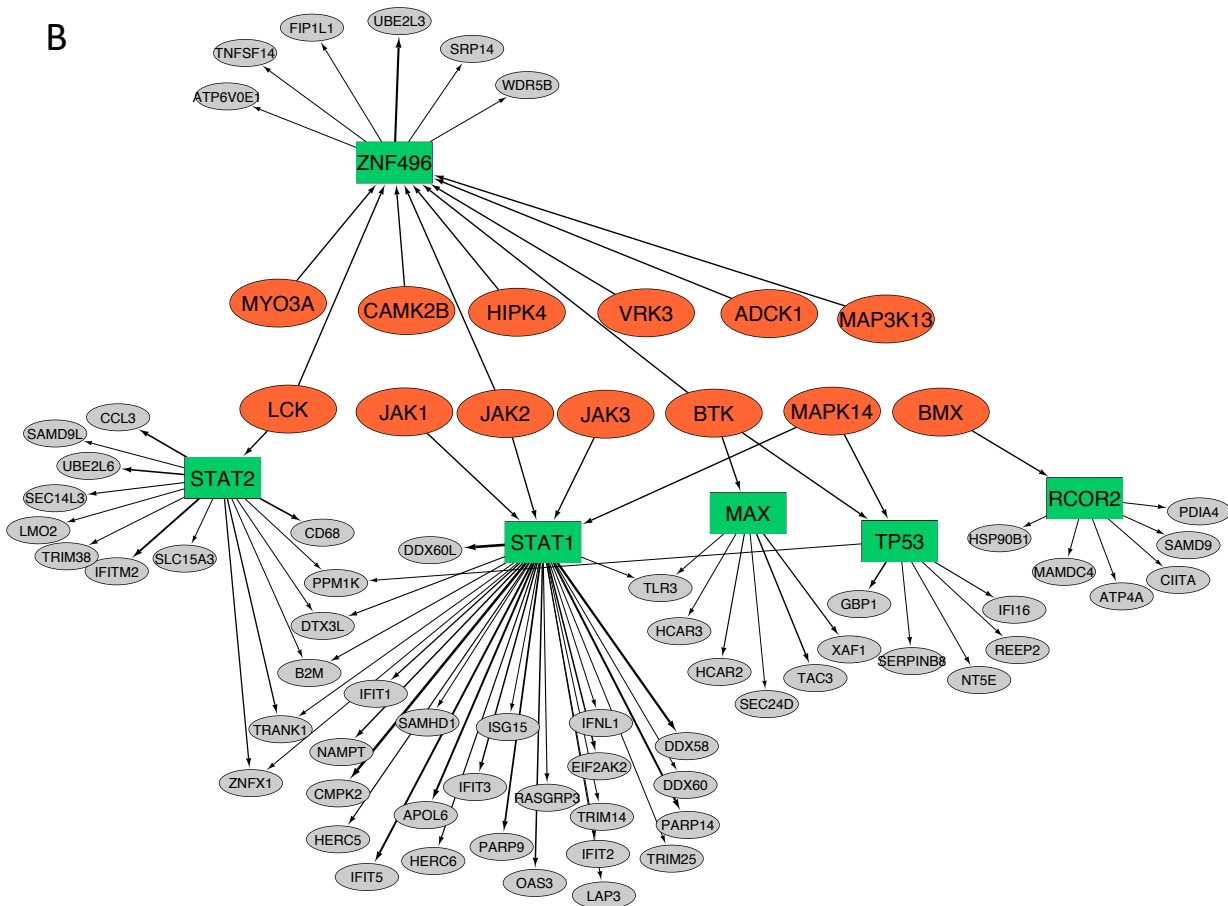
428   **Figure 2:** Network representation of direct interactions between implicated kinases, TFs and genes

429   associated with COVID-19. Kinases are depicted as orange ellipses, TFs are depicted as green rectangles

430   and target genes are depicted as grey ellipses. Only direct kinase-TF interactions present in the

431   aggregated KSI are depicted. A) Network corresponding to the SvM analysis. B) Network corresponding

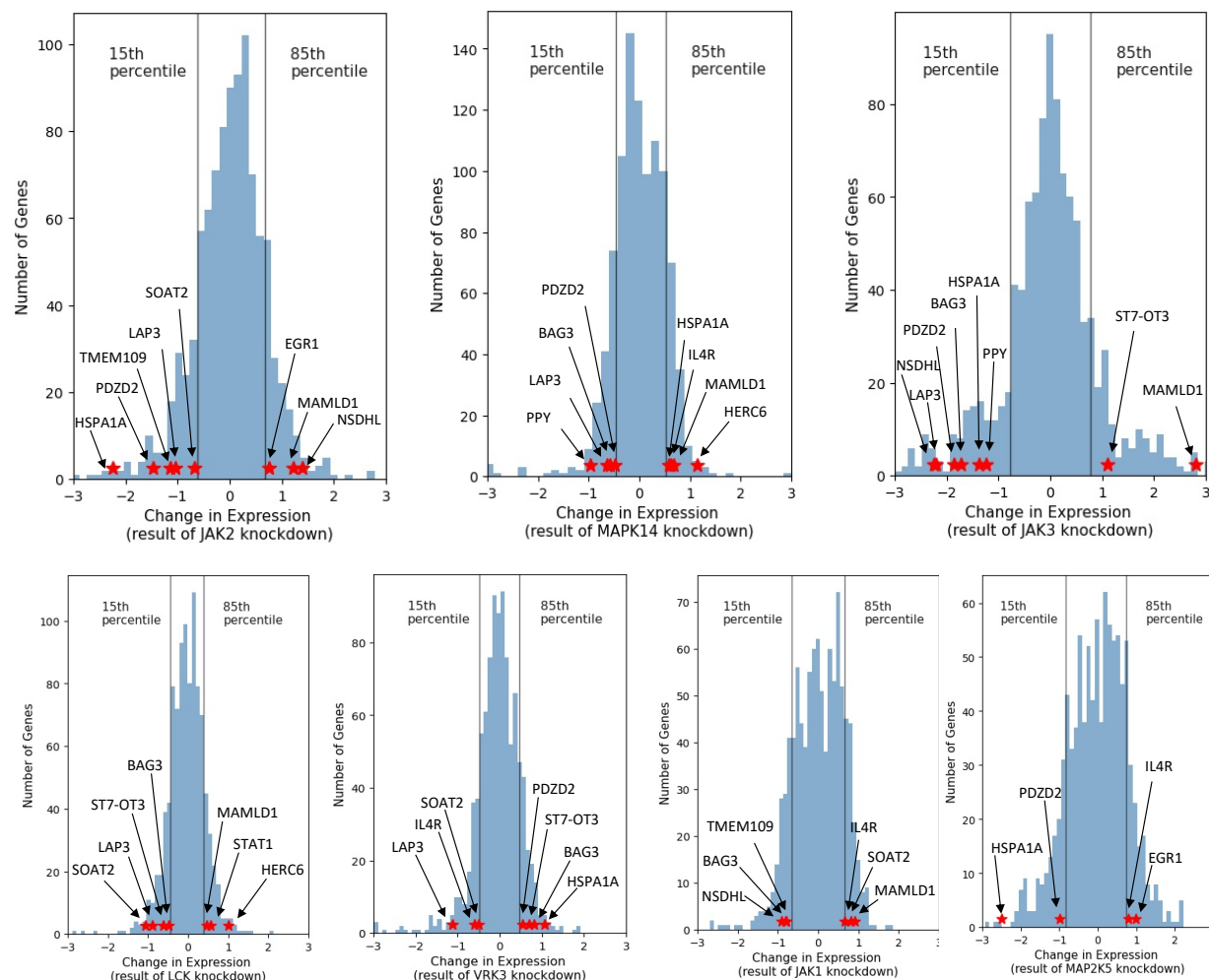432   to the SvOV analysis.

433

434

435

24

436   **Figure 3:** Network representation of indirect interactions between implicated kinases, substrates, TFs

437   and genes associated with COVID-19. Kinases are depicted as orange ellipses, substrates that interact

438   with at least one of the implicated TFs in the HumanNet integrated network are depicted as blue

439   ellipses, TFs are depicted as green rectangles and target genes are depicted as grey ellipses. Directed

440   edges show interactions between kinases and their substrates (obtained from the aggregated KSI) as

441   well as TFs and their target genes (obtained using InPheRNo). Undirected edges correspond to

442   interactions between substrates and TFs (obtained from HumanNet Integrated network). A) Network

443   corresponding to the SvM analysis. B) Network corresponding to the SvOV analysis.

444

445

Figure 4: The histogram of z-score normalized gene expression changes of LINCS L1000 landmark genes in A549 cells as a result of knockdown of kinases implicated in the SvOV analysis. Each histogram corresponds to the knockdown of one kinase. Vertical lines depict the 15th and 85th percentiles and red stars show the TFs and target genes in the SvOV network that are positively or negatively influenced by the experiment.

26

454 **Titles of Supplementary Files:**

455 **Supplementary Figure S1:** The histogram of z-score normalized gene expression changes of LINCS L1000

456 landmark genes in A549 cells as a result of knockdown of kinases implicated in the SvM analysis. Each

457 histogram corresponds to the knockdown of one kinase. Vertical lines depict the 15th and 85th

458 percentiles and red stars show the TFs and target genes in the SvM network that are positively or

459 negatively influenced by the experiment.

460

461 **Supplementary Figure S2:** The effect of kinase knockdowns on genes and TFs shared between the SvM

462 TRN and L1000 landmark genes. An upward arrow shows that the expression of the gene in A549 cells

463 increased and the change in the expression was among the top 15% of all landmark genes. A downward

464 arrow shows that the expression of the gene in A549 cells decreased and the change in the expression

465 was among the bottom 15% of all landmark genes.

466

467 **Supplementary Figure S3:** The effect of kinase knockdowns on genes and TFs shared between the SvOV

468 TRN and L1000 landmark genes. An upward arrow shows that the expression of the gene in A549 cells

469 increased and the change in the expression was among the top 15% of all landmark genes. A downward

470 arrow shows that the expression of the gene in A549 cells decreased and the change in the expression

471 was among the bottom 15% of all landmark genes.

472

473 **Supplementary Table S1**: Top 500 differentially expressed genes and their corresponding p-values. First

474 tab corresponds to genes differentially expressed between SARS-CoV-2 infected cells and mock-treated

475 cells. The second tab corresponds to genes differentially expressed between SARS-CoV-2 infected cells

476 and cells infected by other respiratory viruses.

477

478 **Supplementary Table S2**: The SvM and SvOV TRNs constructed using InPheRNo. Column headers

479 correspond to TFs and row names correspond to target genes. Each entry in the matrix reflects the score

480 assigned to each potential TF-gene edge. Only edges with score > 0.5 were considered for the follow-up

481 analysis.

482

483 **Supplementary Table S3**: The full list of TFs ranked based on the number of COVID-19-relevant target

484 genes identified by InPheRNo in the SvM and SvOV networks.

485

486 **Supplementary Table S4**: Results of standard and network-guided pathway enrichment analysis using

487 KnowEnG's GSC computational pipeline. The results of the first two tabs are obtained by selecting the

488 top 8 TFs from the SvM network as the query gene set, while the results of the last two tabs are

489 obtained by selecting the top 21 TFs from the SvOV network as the query gene set.

490

491 **Supplementary Table S5**: Network-guided pathway enrichment analysis corresponding to TFs and target

492 genes identified by InPheRNo in the SvM network. The results of each tab are obtained by using an

493 implicated TF and its identified target genes as a query gene-set.

494

495 **Supplementary Table S6**: Network-guided pathway enrichment analysis corresponding to TFs and target

496 genes identified by InPheRNo in the SvOV network. The results of each tab are obtained by using an

497 implicated TF and its identified target genes as a query gene-set.

498

499 **Supplementary Table S7**: The full ranked list of kinases identified by foRWaRD for the SvM and SvOV

500 networks.

501

502   **Supplementary Table S8**: The indirect interactions of the implicated kinases and TFs in the SvM and

503   SvOV networks corresponding to Fig. 3. The kinase-substrate relationships are directly extracted from

504   the aggregated KSI. The substrate-TF interactions correspond to edges in the HumanNet Integrated

505   network.

506

507   **Supplementary Table S9**: The effect of shRNA knockdown of implicated kinases on the TFs and target

508   genes identified by InPheRNo in A549 cells. Each tab includes the z-score normalized changes in the

509   expression of the genes as well as the percentile of that change among all L1000 landmark genes.

510

REFERENCES:

512   1. Zhu N, Zhang D, Wang W, Li X, Yang B, Song J, et al. A Novel Coronavirus from Patients with
513   Pneumonia in China, 2019. N Engl J Med. 2020;382(8):727-33. Epub 2020/01/25. doi:
514   10.1056/NEJMoa2001017. PubMed PMID: 31978945; PubMed Central PMCID: PMCPMC7092803.
515   2. Handfield C, Kwock J, MacLeod AS. Innate Antiviral Immunity in the Skin. Trends Immunol.
516   2018;39(4):328-40. Epub 2018/03/13. doi: 10.1016/j.it.2018.02.003. PubMed PMID: 29526487; PubMed
517   Central PMCID: PMCPMC5993211.
518   3. Robert D, Verbiest D, Demey H, Ieven M, Jansens H, Jorens PG. A series of five adult cases of
519   respiratory syncytial virus-related acute respiratory distress syndrome. Anaesth Intensive Care.
520   2008;36(2):230-4. Epub 2008/03/26. doi: 10.1177/0310057X0803600214. PubMed PMID: 18361015.
521   4. Blanco-Melo D, Nilsson-Payant BE, Liu WC, Uhl S, Hoagland D, Moller R, et al. Imbalanced Host
522   Response to SARS-CoV-2 Drives Development of COVID-19. Cell. 2020;181(5):1036-45 e9. Epub
523   2020/05/18. doi: 10.1016/j.cell.2020.04.026. PubMed PMID: 32416070; PubMed Central PMCID:
524   PMCPMC7227586.
525   5. Bem RA, Kneyber MC, van Woensel JB. Respiratory syncytial virus-induced paediatric ARDS: why we
526   should unpack the syndrome. Lancet Respir Med. 2017;5(1):9-10. Epub 2016/12/22. doi:
527   10.1016/S2213-2600(16)30425-8. PubMed PMID: 28000595.
528   6. Henrickson KJ. Parainfluenza viruses. Clin Microbiol Rev. 2003;16(2):242-64. Epub 2003/04/15. doi:
529   10.1128/cmr.16.2.242-264.2003. PubMed PMID: 12692097; PubMed Central PMCID: PMCPMC153148.
530   7. Emad A, Sinha S. Inference of phenotype-relevant transcriptional regulatory networks elucidates
531   cancer type-specific regulatory mechanisms in a pan-cancer study. To appear in NPJ Systems Biology and
532   Applications, bioRxiv. 2018:389734. doi: 10.1101/389734.
533   8. Subramanian A, Narayan R, Corsello SM, Peck DD, Natoli TE, Lu X, et al. A Next Generation
534   Connectivity Map: L1000 Platform and the First 1,000,000 Profiles. Cell. 2017;171(6):1437-52 e17. Epub
535   2017/12/02. doi: 10.1016/j.cell.2017.10.049. PubMed PMID: 29195078; PubMed Central PMCID:
536   PMCPMC5990023.

537   9. Yevshin I, Sharipov R, Kolmykov S, Kondrakhin Y, Kolpakov F. GTRD: a database on gene transcription
538   regulation-2019 update. Nucleic Acids Res. 2019;47(D1):D100-D5. Epub 2018/11/18. doi:
539   10.1093/nar/gky1128. PubMed PMID: 30445619; PubMed Central PMCID: PMCPMC6323985.
540   10. Vishnubalaji R, Shaath H, Alajez NM. Protein Coding and Long Noncoding RNA (lncRNA)
541   Transcriptional Landscape in SARS-CoV-2 Infected Bronchial Epithelial Cells Highlight a Role for
542   Interferon and Inflammatory Response. Genes (Basel). 2020;11(7). Epub 2020/07/11. doi:
543   10.3390/genes11070760. PubMed PMID: 32646047; PubMed Central PMCID: PMCPMC7397219.
544   11. Lokugamage KG, Hage A, de Vries M, Valero-Jimenez AM, Schindewolf C, Dittmann M, et al. Type I
545   Interferon Susceptibility Distinguishes SARS-CoV-2 from SARS-CoV. J Virol. 2020;94(23). Epub
546   2020/09/18. doi: 10.1128/JVI.01410-20. PubMed PMID: 32938761; PubMed Central PMCID:
547   PMCPMC7654262.
548   12. Blatti C, 3rd, Emad A, Berry MJ, Gatzke L, Epstein M, Lanier D, et al. Knowledge-guided analysis of
549   "omics" data using the KnowEnG cloud platform. PLoS Biol. 2020;18(1):e3000583. Epub 2020/01/24.
550   doi: 10.1371/journal.pbio.3000583. PubMed PMID: 31971940; PubMed Central PMCID:
551   PMCPMC6977717.
552   13. Blatti C, Sinha S. Characterizing gene sets using discriminative random walks with restart on
553   heterogeneous biological networks. Bioinformatics. 2016;32(14):2167-75. Epub 2016/05/07. doi:
554   10.1093/bioinformatics/btw151. PubMed PMID: 27153592; PubMed Central PMCID: PMCPMC4937193.
555   14. Szklarczyk D, Gable AL, Lyon D, Junge A, Wyder S, Huerta-Cepas J, et al. STRING v11: protein-protein
556   association networks with increased coverage, supporting functional discovery in genome-wide
557   experimental datasets. Nucleic Acids Res. 2019;47(D1):D607-D13. Epub 2018/11/27. doi:
558   10.1093/nar/gky1131. PubMed PMID: 30476243; PubMed Central PMCID: PMCPMC6323986.
559   15. Fabregat A, Korninger F, Viteri G, Sidiropoulos K, Marin-Garcia P, Ping P, et al. Reactome graph
560   database: Efficient access to complex pathway data. PLoS Comput Biol. 2018;14(1):e1005968. Epub
561   2018/01/30. doi: 10.1371/journal.pcbi.1005968. PubMed PMID: 29377902; PubMed Central PMCID:
562   PMCPMC5805351.
563   16. Cohen P. Protein kinases--the major drug targets of the twenty-first century? Nat Rev Drug Discov.
564   2002;1(4):309-15. Epub 2002/07/18. doi: 10.1038/nrd773. PubMed PMID: 12120282.
565   17. Hornbeck PV, Kornhauser JM, Tkachev S, Zhang B, Skrzypek E, Murray B, et al. PhosphoSitePlus: a
566   comprehensive resource for investigating the structure and function of experimentally determined post-
567   translational modifications in man and mouse. Nucleic Acids Res. 2012;40(Database issue):D261-70.
568   Epub 2011/12/03. doi: 10.1093/nar/gkr1122. PubMed PMID: 22135298; PubMed Central PMCID:
569   PMCPMC3245126.
570   18. Hu J, Rho HS, Newman RH, Zhang J, Zhu H, Qian J. PhosphoNetworks: a database for human
571   phosphorylation networks. Bioinformatics. 2014;30(1):141-2. Epub 2013/11/15. doi:
572   10.1093/bioinformatics/btt627. PubMed PMID: 24227675; PubMed Central PMCID: PMCPMC3866559.
573   19. Cheng F, Jia P, Wang Q, Zhao Z. Quantitative network mapping of the human kinome interactome
574   reveals new clues for rational kinase inhibitor discovery and individualized cancer therapy. Oncotarget.
575   2014;5(11):3697-710. Epub 2014/07/09. doi: 10.18632/oncotarget.1984. PubMed PMID: 25003367;
576   PubMed Central PMCID: PMCPMC4116514.
577   20. Ding J, Hostallero DE, El Khili MR, Fonseca GJ, Milette S, Noorah N, et al. A network-informed analysis
578   of SARS-CoV-2 and hemophagocytic lymphohistiocytosis genes' interactions points to Neutrophil
579   Extracellular Traps as mediators of thrombosis in COVID-19. medRxiv. 2020:2020.07.01.20144121. doi:
580   10.1101/2020.07.01.20144121.
581   21. Hwang S, Kim CY, Yang S, Kim E, Hart T, Marcotte EM, et al. HumanNet v2: human gene networks for
582   disease research. Nucleic Acids Res. 2019;47(D1):D573-D80. Epub 2018/11/13. doi:
583   10.1093/nar/gky1126. PubMed PMID: 30418591; PubMed Central PMCID: PMCPMC6323914.

584   22. Yamaoka K, Saharinen P, Pesu M, Holt VE, 3rd, Silvennoinen O, O'Shea JJ. The Janus kinases (Jaks).
585   Genome Biol. 2004;5(12):253. Epub 2004/12/04. doi: 10.1186/gb-2004-5-12-253. PubMed PMID:
586   15575979; PubMed Central PMCID: PMCPMC545791.
587   23. Luo W, Li YX, Jiang LJ, Chen Q, Wang T, Ye DW. Targeting JAK-STAT Signaling to Control Cytokine
588   Release Syndrome in COVID-19. Trends Pharmacol Sci. 2020;41(8):531-43. Epub 2020/06/26. doi:
589   10.1016/j.tips.2020.06.007. PubMed PMID: 32580895; PubMed Central PMCID: PMCPMC7298494.
590   24. Seif F, Aazami H, Khoshmirsafa M, Kamali M, Mohsenzadegan M, Pornour M, et al. JAK Inhibition as a
591   New Treatment Strategy for Patients with COVID-19. Int Arch Allergy Immunol. 2020;181(6):467-75.
592   Epub 2020/05/12. doi: 10.1159/000508247. PubMed PMID: 32392562; PubMed Central PMCID:
593   PMCPMC7270061.
594   25. Goker Bagca B, Biray Avci C. The potential of JAK/STAT pathway inhibition by ruxolitinib in the
595   treatment of COVID-19. Cytokine Growth Factor Rev. 2020;54:51-62. Epub 2020/07/09. doi:
596   10.1016/j.cytogfr.2020.06.013. PubMed PMID: 32636055; PubMed Central PMCID: PMCPMC7305753.
597   26. Mehta P, McAuley DF, Brown M, Sanchez E, Tattersall RS, Manson JJ, et al. COVID-19: consider
598   cytokine storm syndromes and immunosuppression. Lancet. 2020;395(10229):1033-4. Epub
599   2020/03/21. doi: 10.1016/S0140-6736(20)30628-0. PubMed PMID: 32192578; PubMed Central PMCID:
600   PMCPMC7270045.
601   27. Li Q, Wu J, Nie J, Zhang L, Hao H, Liu S, et al. The Impact of Mutations in SARS-CoV-2 Spike on Viral
602   Infectivity and Antigenicity. Cell. 2020;182(5):1284-94 e9. Epub 2020/07/31. doi:
603   10.1016/j.cell.2020.07.012. PubMed PMID: 32730807; PubMed Central PMCID: PMCPMC7366990.
604   28. Hadjadj J, Yatim N, Barnabei L, Corneau A, Boussier J, Smith N, et al. Impaired type I interferon
605   activity and inflammatory responses in severe COVID-19 patients. Science. 2020;369(6504):718-24. Epub
606   2020/07/15. doi: 10.1126/science.abc6027. PubMed PMID: 32661059; PubMed Central PMCID:
607   PMCPMC7402632.
608   29. Sallard E, Lescure FX, Yazdanpanah Y, Mentre F, Peiffer-Smadja N. Type 1 interferons as a potential
609   treatment against COVID-19. Antiviral Res. 2020;178:104791. Epub 2020/04/11. doi:
610   10.1016/j.antiviral.2020.104791. PubMed PMID: 32275914; PubMed Central PMCID: PMCPMC7138382.
611   30. Park A, Iwasaki A. Type I and Type III Interferons - Induction, Signaling, Evasion, and Application to
612   Combat COVID-19. Cell Host Microbe. 2020;27(6):870-8. Epub 2020/05/29. doi:
613   10.1016/j.chom.2020.05.008. PubMed PMID: 32464097; PubMed Central PMCID: PMCPMC7255347.
614   31. Chen G, Wu D, Guo W, Cao Y, Huang D, Wang H, et al. Clinical and immunological features of severe
615   and moderate coronavirus disease 2019. J Clin Invest. 2020;130(5):2620-9. Epub 2020/03/29. doi:
616   10.1172/JCI137244. PubMed PMID: 32217835; PubMed Central PMCID: PMCPMC7190990.
617   32. Hernandez N, Melki I, Jing H, Habib T, Huang SSY, Danielson J, et al. Life-threatening influenza
618   pneumonitis in a child with inherited IRF9 deficiency. J Exp Med. 2018;215(10):2567-85. Epub
619   2018/08/26. doi: 10.1084/jem.20180628. PubMed PMID: 30143481; PubMed Central PMCID:
620   PMCPMC6170168.
621   33. van der Made CI, Simons A, Schuurs-Hoeijmakers J, van den Heuvel G, Mantere T, Kersten S, et al.
622   Presence of Genetic Variants Among Young Men With Severe COVID-19. JAMA. 2020. Epub 2020/07/25.
623   doi: 10.1001/jama.2020.13719. PubMed PMID: 32706371; PubMed Central PMCID: PMCPMC7382021.
624   34. Zhang Q, Bastard P, Liu Z, Le Pen J, Moncada-Velez M, Chen J, et al. Inborn errors of type I IFN
625   immunity in patients with life-threatening COVID-19. Science. 2020;370(6515). Epub 2020/09/26. doi:
626   10.1126/science.abd4570. PubMed PMID: 32972995.
627   35. Brunetta E, Folci M, Bottazzi B, De Santis M, Gritti G, Protti A, et al. Macrophage expression and
628   prognostic significance of the long pentraxin PTX3 in COVID-19. Nat Immunol. 2021;22(1):19-24. Epub
629   2020/11/20. doi: 10.1038/s41590-020-00832-x. PubMed PMID: 33208929.

630   36. Lammermann T, Kastenmuller W. Concepts of GPCR-controlled navigation in the immune system.
631   Immunol Rev. 2019;289(1):205-31. Epub 2019/04/13. doi: 10.1111/imr.12752. PubMed PMID:
632   30977203; PubMed Central PMCID: PMCPMC6487968.
633   37. Grimes JM, Grimes KV. p38 MAPK inhibition: A promising therapeutic approach for COVID-19. J Mol
634   Cell Cardiol. 2020;144:63-5. Epub 2020/05/19. doi: 10.1016/j.yjmcc.2020.05.007. PubMed PMID:
635   32422320; PubMed Central PMCID: PMCPMC7228886.
636   38. Kopecky-Bromberg SA, Martinez-Sobrido L, Palese P. 7a protein of severe acute respiratory
637   syndrome coronavirus inhibits cellular protein synthesis and activates p38 mitogen-activated protein
638   kinase. J Virol. 2006;80(2):785-93. Epub 2005/12/28. doi: 10.1128/JVI.80.2.785-793.2006. PubMed
639   PMID: 16378980; PubMed Central PMCID: PMCPMC1346853.
640   39. Bouhaddou M, Memon D, Meyer B, White KM, Rezelj VV, Correa Marrero M, et al. The Global
641   Phosphorylation Landscape of SARS-CoV-2 Infection. Cell. 2020;182(3):685-712 e19. Epub 2020/07/10.
642   doi: 10.1016/j.cell.2020.06.034. PubMed PMID: 32645325; PubMed Central PMCID: PMCPMC7321036.
643   40. Berube J, Bourdon C, Yao Y, Rousseau S. Distinct intracellular signaling pathways control the
644   synthesis of IL-8 and RANTES in TLR1/TLR2, TLR3 or NOD1 activated human airway epithelial cells. Cell
645   Signal. 2009;21(3):448-56. Epub 2009/01/06. doi: 10.1016/j.cellsig.2008.12.001. PubMed PMID:
646   19121387.
647   41. Roschewski M, Lionakis MS, Sharman JP, Roswarski J, Goy A, Monticelli MA, et al. Inhibition of
648   Bruton tyrosine kinase in patients with severe COVID-19. Sci Immunol. 2020;5(48). Epub 2020/06/07.
649   doi: 10.1126/sciimmunol.abd0110. PubMed PMID: 32503877; PubMed Central PMCID:
650   PMCPMC7274761.
651   42. Treon SP, Castillo JJ, Skarbnik AP, Soumerai JD, Ghobrial IM, Guerrera ML, et al. The BTK inhibitor
652   ibrutinib may protect against pulmonary injury in COVID-19-infected patients. Blood.
653   2020;135(21):1912-5. Epub 2020/04/18. doi: 10.1182/blood.2020006288. PubMed PMID: 32302379;
654   PubMed Central PMCID: PMCPMC7243149.
655   43. Nicolson PL, Welsh JD, Chauhan A, Thomas MR, Kahn ML, Watson SP. A rationale for blocking
656   thromboinflammation in COVID-19 with Btk inhibitors. Platelets. 2020;31(5):685-90. Epub 2020/06/20.
657   doi: 10.1080/09537104.2020.1775189. PubMed PMID: 32552307.
658   44. Barnes BJ, Adrover JM, Baxter-Stoltzfus A, Borczuk A, Cools-Lartigue J, Crawford JM, et al. Targeting
659   potential drivers of COVID-19: Neutrophil extracellular traps. J Exp Med. 2020;217(6). Epub 2020/04/18.
660   doi: 10.1084/jem.20200652. PubMed PMID: 32302401; PubMed Central PMCID: PMCPMC7161085
661   work. R.E. Schwartz is a Sponsored Advisory Board Member for Miromatrix Inc. J.D. Spicer reported
662   personal fees from Bristol Myers Squibb, personal fees from Astra Zeneca, personal fees from Merck,
663   personal fees from Trans-Hit Bio, and non-financial support from Astra Zeneca outside the submitted
664   work. C.C. Yost reports a grant from PEEL Therapeutics, Inc. during the conduct of the study; in addition,
665   C.C. Yost authors a US patent (patent no. 10,232,023 B2) held by the University of Utah for the use of
666   NET-inhibitory peptides for "treatment of and prophylaxis against inflammatory disorders." PEEL
667   Therapeutics, Inc. has exclusive licensing rights. M. Egeblad reported "other" from Santhera during the
668   conduct of the study; and consulted for CytomX in 2019. No other disclosures were reported.
669   45. Bhattacharyya S, Brown DE, Brewer JA, Vogt SK, Muglia LJ. Macrophage glucocorticoid receptors
670   regulate Toll-like receptor 4-mediated inflammatory responses by selective inhibition of p38 MAP
671   kinase. Blood. 2007;109(10):4313-9. Epub 2007/01/27. doi: 10.1182/blood-2006-10-048215. PubMed
672   PMID: 17255352; PubMed Central PMCID: PMCPMC1885507.
673   46. Group RC, Horby P, Lim WS, Emberson JR, Mafham M, Bell JL, et al. Dexamethasone in Hospitalized
674   Patients with Covid-19 - Preliminary Report. N Engl J Med. 2020. Epub 2020/07/18. doi:
675   10.1056/NEJMoa2021436. PubMed PMID: 32678530; PubMed Central PMCID: PMCPMC7383595.

676   47. Mano H. Tec family of protein-tyrosine kinases: an overview of their structure and function. Cytokine
677   Growth Factor Rev. 1999;10(3-4):267-80. Epub 2000/01/27. doi: 10.1016/s1359-6101(99)00019-2.
678   PubMed PMID: 10647781.
679   48. Semaan N, Alsaleh G, Gottenberg JE, Wachsmann D, Sibilia J. Etk/BMX, a Btk family tyrosine kinase,
680   and Mal contribute to the cross-talk between MyD88 and FAK pathways. J Immunol. 2008;180(5):3485-
681   91. Epub 2008/02/23. doi: 10.4049/jimmunol.180.5.3485. PubMed PMID: 18292575.
682   49. Zhu L, Yang P, Zhao Y, Zhuang Z, Wang Z, Song R, et al. Single-Cell Sequencing of Peripheral
683   Mononuclear Cells Reveals Distinct Immune Response Landscapes of COVID-19 and Influenza Patients.
684   Immunity. 2020;53(3):685-96 e3. Epub 2020/08/14. doi: 10.1016/j.immuni.2020.07.009. PubMed PMID:
685   32783921; PubMed Central PMCID: PMCPMC7368915.
686   50. Tamada K, Shimozaki K, Chapoval AI, Zhai Y, Su J, Chen SF, et al. LIGHT, a TNF-like molecule,
687   costimulates T cell proliferation and is required for dendritic cell-mediated allogeneic T cell response. J
688   Immunol. 2000;164(8):4105-10. Epub 2001/02/07. doi: 10.4049/jimmunol.164.8.4105. PubMed PMID:
689   10754304.
690   51. Leaman DW, Chawla-Sarkar M, Vyas K, Reheman M, Tamai K, Toji S, et al. Identification of X-linked
691   inhibitor of apoptosis-associated factor-1 as an interferon-stimulated gene that augments TRAIL Apo2L-
692   induced apoptosis. J Biol Chem. 2002;277(32):28504-11. Epub 2002/05/25. doi:
693   10.1074/jbc.M204851200. PubMed PMID: 12029096.
694   52. Zhang HM, Liu T, Liu CJ, Song S, Zhang X, Liu W, et al. AnimalTFDB 2.0: a resource for expression,
695   prediction and functional study of animal transcription factors. Nucleic Acids Res. 2015;43(Database
696   issue):D76-81. doi: 10.1093/nar/gku887. PubMed PMID: 25262351; PubMed Central PMCID:
697   PMCPMC4384004.
698   53. Smith I, Greenside PG, Natoli T, Lahr DL, Wadden D, Tirosh I, et al. Evaluation of RNAi and CRISPR
699   technologies by large-scale gene expression profiling in the Connectivity Map. PLoS Biol.
700   2017;15(11):e2003213. Epub 2017/12/01. doi: 10.1371/journal.pbio.2003213. PubMed PMID:
701   29190685; PubMed Central PMCID: PMCPMC5726721.
702   54. Robinson MD, McCarthy DJ, Smyth GK. edgeR: a Bioconductor package for differential expression
703   analysis of digital gene expression data. Bioinformatics. 2010;26(1):139-40. Epub 2009/11/17. doi:
704   10.1093/bioinformatics/btp616. PubMed PMID: 19910308; PubMed Central PMCID: PMCPMC2796818.
705   55. Law CW, Chen Y, Shi W, Smyth GK. voom: Precision weights unlock linear model analysis tools for
706   RNA-seq read counts. Genome Biol. 2014;15(2):R29. Epub 2014/02/04. doi: 10.1186/gb-2014-15-2-r29.
707   PubMed PMID: 24485249; PubMed Central PMCID: PMCPMC4053721.
708